Reference: *Biol. Bull.* **203:** 27–41. (August 2002)

Anatomical Correlates of Venom Production in *Conus californicus*

JENNIFER MARSHALL[1], WAYNE P. KELLEY[2], STANISLAV S. RUBAKHIN[2], JON-PAUL BINGHAM[3], JONATHAN V. SWEEDLER[2], AND WILLIAM F. GILLY[1,*]

[1]*Hopkins Marine Station and Department of Biological Sciences of Stanford University, Pacific Grove, California 93950;* [2]*Department of Chemistry and the Beckman Institute, University of Illinois, Urbana, Illinois 61801; and* [3]*Department of Pharmacology, Yale University School of Medicine, New Haven, Connecticut 06520*

Abstract. Like all members of the genus, *Conus californicus* has a specialized venom apparatus, including a modified radular tooth, with which it injects paralyzing venom into its prey. In this paper the venom duct and its connection to the pharynx, along with the radular sac and teeth, were examined using light and transmission electron microscopy. The general anatomy of the venom apparatus resembles that in other members of the genus, but several features are described that have not been previously reported for other species. The proximal (posterior) quarter of the venom duct is composed of a complex epithelium that may be specialized for active transport rather than secretion. The distal portion of the duct is composed of a different type of epithelium, suggestive of holocrine secretion, and the cells display prominent intracellular granules of at least two types. Similar granules fill the lumen of the duct. The passageway between the lumen of the venom duct and pharynx is a flattened branching channel that narrows to a width of 10 μm and is lined by a unique cell type of unknown function. Granular material similar to that in the venom duct was also found in the lumen of individual teeth within the radular sac. Mass spectrometry (MALDI-TOF) demonstrated the presence of putative peptides in material derived from the tooth lumen, and all of the more prominent species were also evident in the anterior venom duct. Radular teeth thus appear to be loaded with peptide toxins while they are still in the radular sac.

Received 26 October 2001; accepted 25 June 2002.

* To whom correspondence should be addressed. E-mail: lignje@stanford.edu

Abbreviations: MALDI-TOF, matrix-assisted laser desorption-ionization time of flight mass spectrometry; *m/z*, mass-to-charge ratio.

Introduction

Predatory marine snails of the genus *Conus* have long been of interest because their highly evolved hunting strategies employ peptide toxins that paralyze prey (Bergh, 1895; Shaw, 1914; Kohn, 1956; reviewed by Halstead, 1988). The gastropod radula is typically equipped with rows of chitinous teeth that scrape or bite during feeding. In cone snails, however, the radular teeth are unattached and resemble barbed hypodermic needles that are used to inject venom into the prey. When resting, the snail holds its proboscis retracted inside the rostrum. When prey is sensed by waterborne chemical signals (Spengler and Kohn, 1995), searching behavior commences with the proboscis extended and a tooth held near the tip by a sphincter (Kohn, 1956; Greene and Kohn, 1989). When prey is contacted, the tooth is forcibly inserted into the victim, and venom is injected.

Each of the more than 500 *Conus* species (Röckel *et al.*, 1995; Kohn, 1998) is thought to contain a large number of distinct peptide toxins in the venom duct (Olivera, 1997; McIntosh *et al.*, 1999), and contemporary *Conus* research has primarily focused on purifying and characterizing these toxins. *Conus* toxins are typically 10–30 amino acids in length and belong to one of several families defined by highly conserved cysteine frameworks and internal disulfide linkages (Olivera *et al.*, 1995; McIntosh *et al.*, 1999; Duda and Palumbi, 1999; Conticello *et al.*, 2001). Most of these peptides target voltage- and ligand-gated ion channels.

Production and delivery of *Conus* venom involves three general steps: (1) synthesis, processing, and packaging of peptide toxins; (2) generation and storage of radular teeth and transfer of a tooth to the tip of the proboscis; and (3) the final insertion of the tooth and ejection of venom. These

processes are carried out within an anatomically complex venom apparatus in conjunction with the anterior regions of the digestive tract. These features are relatively invariable between *Conus* species (see Halstead, 1988), and a schematic venom apparatus is illustrated in Figure 1.

Some events listed above can be assigned to specific anatomical components:

1. Production of venom takes place in a long, convoluted venom duct. The proximal end of the duct is equipped with a muscular bulb. Distally the duct enters the pharynx just anterior to its border with the esophagus. Proximal and distal portions of the duct differ in gross structure and venom content (Endean and Duchemin, 1967; Bingham *et al.,* 1996), but the sites of synthesis, post-translational modification, and presumed packaging of peptides into large "venom granules" (Maguire and Kwan, 1992) remain unclear. Although these granules are undoubtedly associated with toxin production, there is no compelling evidence that they contain active peptides.
2. Teeth are generated in the long arm of the radular sac, and mature teeth are stored in the short arm, the lumen of which enters the pharynx slightly anterior to the venom duct opening (Marsh, 1977). In preparation for use, an individual tooth is transported into the pharynx by an unknown mechanism, where it is probably surrounded by the retracted proboscis and then grasped around the basal spur by a subterminal sphincter (Hermitte, 1946; Greene and Kohn, 1989). At this point, the lumen of the tooth is thought to be empty (Marsh, 1977) and ready to be filled with venom that has moved into the pharynx directly from the venom duct (Kohn *et al.,* 1960). Finally, the proboscis extends with the venom-loaded tooth held at the tip.
3. The muscular bulb is generally thought to take little or no part in the secretion of venom (see Halstead, 1988). Although the bulb has often been hypothesized to provide the force for final venom ejection out of the tooth (see Halstead, 1988; Endean and Duchemin, 1967; Freeman *et al.,* 1974; Olivera, 1997), there is no direct evidence for this idea. It is more likely that the muscular proboscis provides the necessary positive pressure to mediate venom ejection (Songdahl, 1973; Greene and Kohn, 1989; Kohn and Hunter, 2001). The mechanics of this action are unclear, and the function of the muscular bulb remains enigmatic.

We have been studying the biology of venom production in *Conus californicus,* a local species. Toxic components exist in the venom, but they have not been studied in detail (Whysner and Saunders, 1963, 1966; Cottrell and Twarog, 1972; Elliot and Kehoe, 1978; Elliot and Raftery, 1979; Bingham *et al.,* 2000). Anatomical studies are also limited

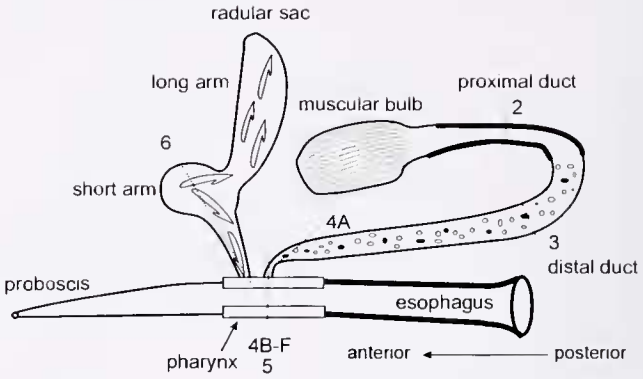

Figure 1. Schematic representation of the main parts of a generic *Conus* venom apparatus and the anterior digestive tract. The figure is not to scale. Only a few of the many teeth are indicated in the short and long arms of the radular sac. Numbered dotted lines indicate the approximate position and orientation of the sections described in Figures 2–6.

(Hinegardner, 1958; Halstead, 1988), and cellular details that might be correlated with biochemical data are lacking.

This report describes some new features of the venom apparatus in *C. californicus* as revealed by conventional light and transmission electron microscopy. First, we have found that the proximal portion of the venom duct has a unique structure and may be specialized for active transport rather than secretion. Second, we have discovered a novel and unusually narrow passageway between the venom duct and the pharynx through which venom must pass prior to ejection. Third, complex, granular material resembling that in the lumen of the venom duct is found packaged inside the lumen of individual teeth while they are still in the radular sac. Furthermore, mass spectrometry demonstrates that presumptive peptides can be identified in material isolated from the venom duct and from the lumen of single radular teeth. Although the sequences of these peptides are unknown, equivalence in their apparent molecular weights suggests that some of the same peptides are present in both locations.

Materials and Methods

Specimens of *Conus californicus* were obtained from Monterey Bay, California (Sea Life Supply, Sand City, CA), and maintained in the laboratory for as long as several weeks in a flow-through seawater system (13–15°C) or in an aerated, closed system at room temperature (22–24°C). Results obtained from the two sets of animals were equivalent.

Light and electron microscopy

In preparation for light microscopy, two animals were relaxed in seawater containing 2% $MgCl_2$, and the shells were cracked with vise-grips and removed. The complete venom apparatus and anterior digestive tract as depicted in Figure 1 were dissected under seawater. Tissue samples

were fixed overnight at 4°C in 2% glutaraldehyde made up in 80% filtered seawater containing 100 m*M* HEPES (pH 7.3) and then dehydrated in a graded ethanol series. Tissues were then cut into smaller pieces (several cubic millimeters) and embedded in Spurs resin. Sections (0.5–2 μm) were cut with an ultramicrotome equipped with a glass knife, stained with 1% methylene blue dissolved in 0.1 N NaOH, and examined with an Olympus BH-2 microscope. The venom duct was examined at several places along its length, and anatomical locations and orientations of all sections figured in this paper are indicated in Figure 1.

For transmission electron microscopy (TEM), tissue was fixed and embedded as described above, except a post-fixation step of 1% OsO_4 in seawater for 1 h was added. Sections were cut with a diamond knife, stained with saturated uranyl acetate and lead citrate in 0.1 N NaOH, and viewed on a Phillips CM12 microscope at Stanford University School of Medicine.

Living animals were also relaxed and dissected as described above to reveal the junction between the short arm of the radular sac and the pharynx. An incision was made at the junction and several teeth were carefully removed with a fine forceps. The teeth were rinsed well in seawater and examined using water immersion optics.

Matrix-assisted laser desorption-ionization time of flight mass spectrometry (MALDI-TOF)

A complete venom apparatus was removed as described above, and the distalmost thin segment of venom duct (area 4 in Fig. 1) was ligated with fine surgical silk close to where it enters the pharyngeal wall; this ligation prevents any leakage of venom into the proboscis and potentially into the radular sac. Most of the proboscis and esophagus were removed, and the pharynx was then slit longitudinally and the lumen was washed with seawater. This semi-intact venom duct (with bulb) and radular sac preparation was then shipped in iced seawater to the University of Illinois by overnight carrier.

Individual teeth from the short arm of the radular sac were dissected upon arrival in Illinois and washed well in isotonic NaCl. Single teeth were broken open with forceps and mashed onto a MALDI target into 0.5 μl of matrix solution (10 mg ml^{-1} 2,5-dihydroxybenzoic acid (ICN Pharmaceuticals, Costa Mesa, CA)) in deionized water. Short (~1 mm) segments of the venom duct were also cut from locations corresponding to areas 2, 3, and 4 in Figure 1. Some of the luminal contents of these sections was squeezed into the same volume of matrix solution on additional target spots.

MALDI-TOF MS analysis was carried out as previously described (Sweedler *et al.*, 2000; Li *et al.*, 2000) using a Voyager DE STR (PE Biosystems, Framingham, MA). A pulsed, nitrogen laser (337 nm) served as the desorption/ionization source, and positive-ion mass spectra were obtained with both linear and reflection modes of operation. The former mode has greater sensitivity, whereas the latter is more accurate in establishing mass. Mass-to-charge ratio (*m/z*) calibrations were performed externally with a standard calibration mixture including angiotensin and bovine insulin (Sequazyme, PE Biosystems, Framingham, MA). For data presented in this paper, the *m/z* parameter is equivalent to molecular weight (Bingham *et al.*, 1996). The spectra shown are representative examples from several hundred spectra acquired from several snails.

Results

The proximal venom duct

Near its junction with the muscular bulb, the proximal (*i.e.*, posterior) venom duct, in an animal of 30–35 mm shell-length, is orange-pink and about 250 μm in diameter. Light microscopy reveals three distinct zones in this region (Fig. 2A): an outermost layer of connective tissue (c), a cellular, epithelial layer (ep), and an inner lumen (l).

Electron microscopy (Fig. 2B) shows that the outer layer is composed mostly of collagen-like fibrils (c), which are themselves layered according to their direction of orientation. Scattered profiles of presumptive muscle cells (m) are embedded in the collagen layer and appear to be associated with certain sublayers. This collagen-rich layer is not covered by a distinct outer cellular layer, although cells that are probably fibroblasts can be found on the outer surface.

The inner surface of this collagenous layer is an amorphous basal lamina (see also Fig. 3B) that covers the cellular layer (ep). Cells in this epithelium contain numerous mitochondria (mt, white pointers) that are concentrated on the basal surface facing the collagen layer. Nuclei also tend to be located here (n in Fig. 2A). The apical surface of the epithelial cells is densely covered with microvilli that protrude into the lumen (mv in Fig. 2B). Boundaries between these interdigitating cells are highly complex in this region, and tight junctions are also present along the apical surface (black arrow).

Much cellular debris (cd) and many mitochondrial fragments (mt) are found in the lumen of the duct (Fig. 2C), and this material probably derives from more distal regions of the duct as described below. Profiles of cilia in small clusters are fairly common (arrow), but it is unclear whether they are part of the debris or whether they emerge from cells in the epithelial layer. A few venom granules (g) are found in the lumen, but they are relatively uncommon in this region of the duct.

The distal venom duct

About one-quarter of the distance to the pharynx, the venom duct enlarges to a diameter of about 375 μm and

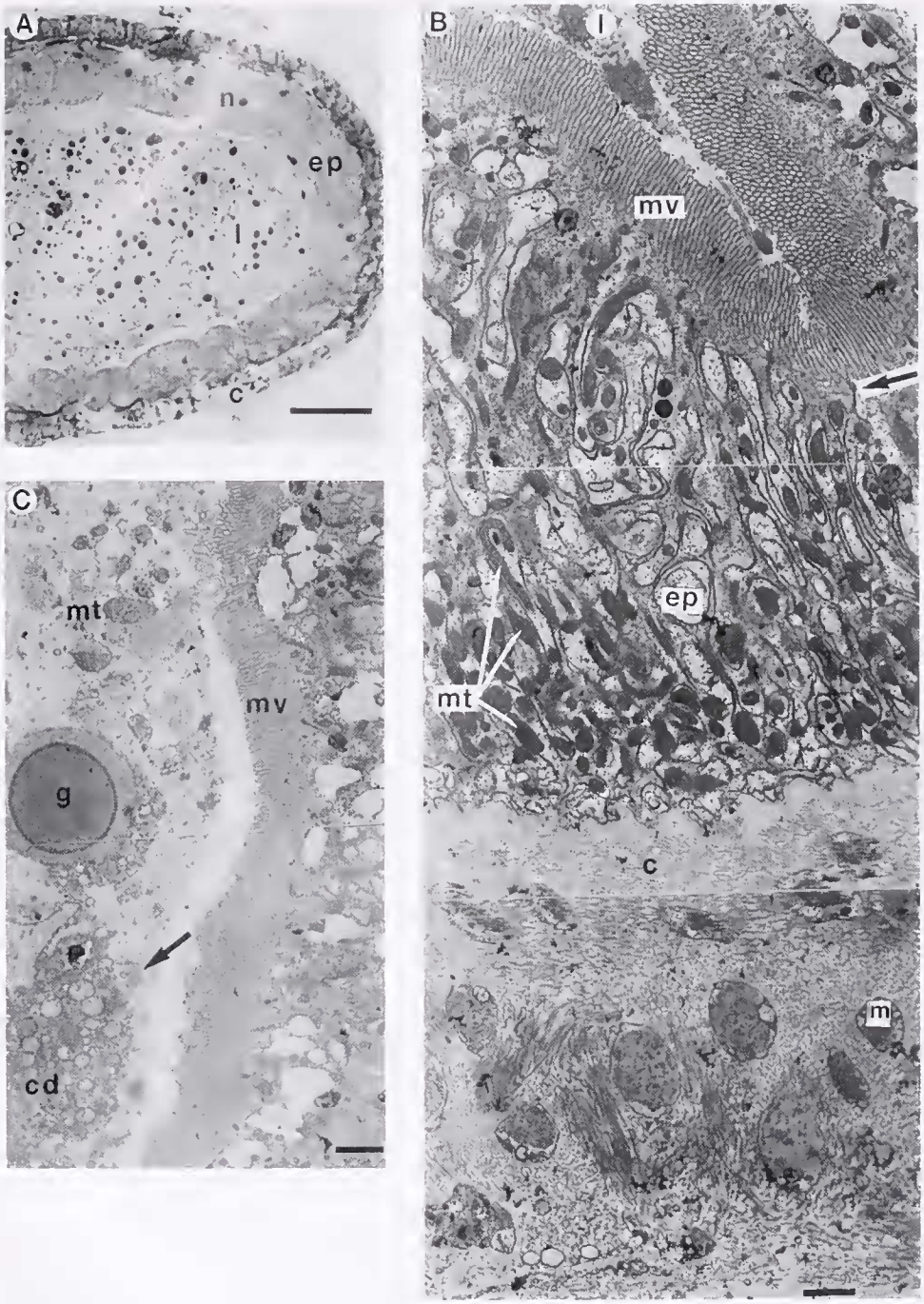

Figure 2. Proximal portion of the venom duct. (A) Low-power light micrograph showing overall view of the duct in this region. A collagenous layer (c) covers an epithelium (ep) composed of large cells with prominent nuclei (n). The lumen (l) contains noncellular material. Scale bar is 50 μm. (B) TEM image of the complete collagenous and epithelial layers. Muscle-cell (m) profiles occur in the collagenous layer; mitochondria (mt) densely pack the basal end of the epithelial cells (ep); and microvilli (mv) cover the apical surfaces. Tight junctions (arrow) exist along this surface. Scale bar is 1 μm. (C) TEM image of apical edge of the epithelial cells and the lumen. There are large amounts of cellular debris (cd) in the lumen and mitochondrial fragments (mt) as well as cross sections of ordinary "9+2" cilia (5 indicated by arrow) and sparse venom granules (g). Scale bar is 1 μm.

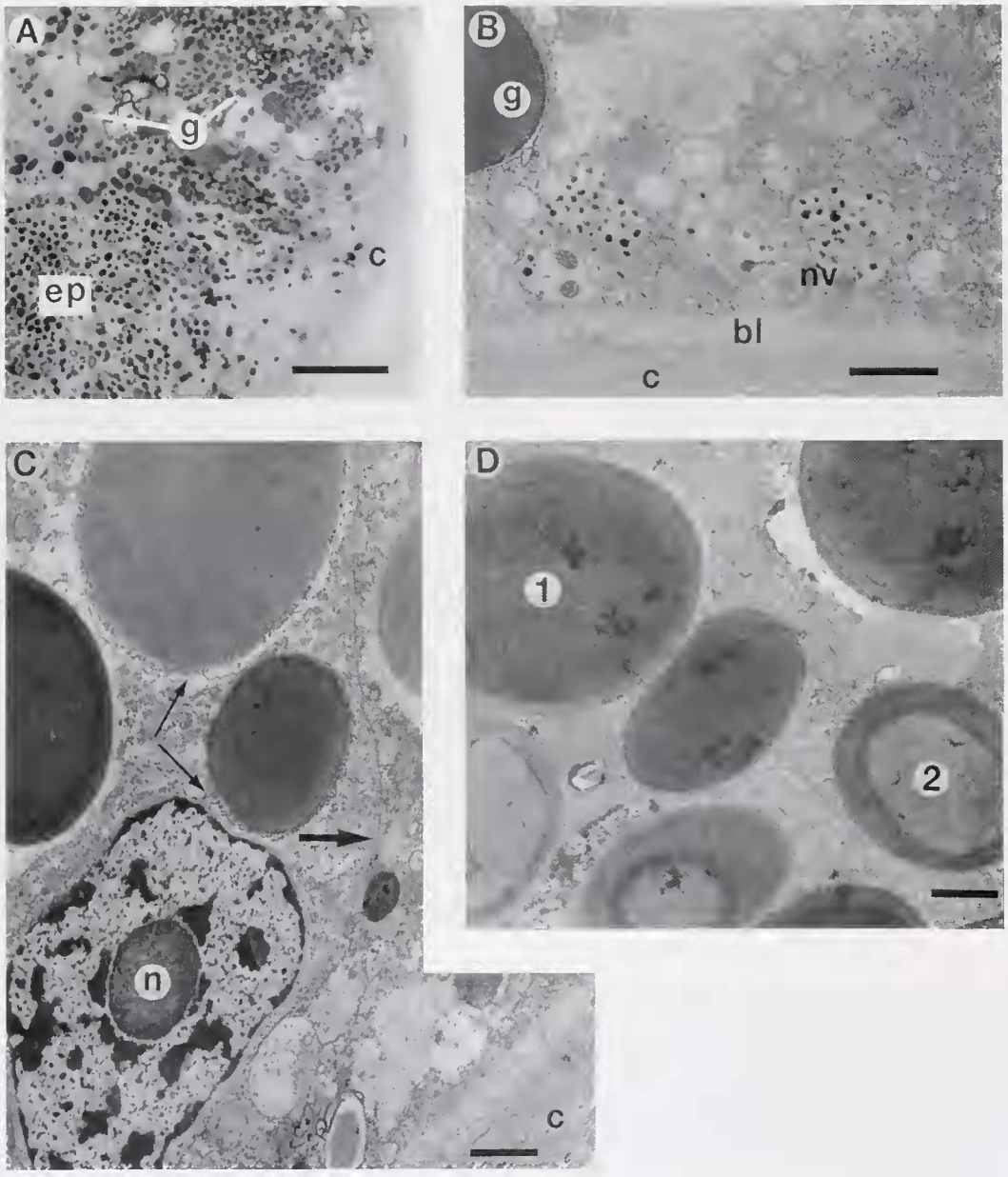

Figure 3. Middle region of the distal venom duct. (A) Light micrograph of the collagenous layer (c) and epithelial cells (ep). Venom granules (g) are prominent. Scale bar is 50 μm. (B) TEM image of the basal surface of epithelial cells, basal lamina (bl), and collagen fibrils (c). Profiles of neural processes (nv) containing dense vesicles are apparent. A portion of a venom granule is visible (g). Scale bar is 1 μm. (C) TEM image of a nucleus (n) and intracellular venom granules. Large arrow points to the cell membrane. Thinner arrows point to the membranous coating of venom granules. Scale bar is 1 μm. (D) TEM image of venom granules of two different types (1 and 2). The area of this section is in the central region of the duct near the lumen, where unambiguous distinction between extracellular and intracellular regions is difficult due to the breakdown of cell membranes associated with secretion. Scale bar is 1 μm.

becomes creamy white. Duct morphology also dramatically changes, as evidenced by the light micrograph in Figure 3A. The outer layer is still collagenous (c), but the nature of the epithelium is quite different. Large, vaguely columnar epithelial cells with poorly demarcated luminal and lateral boundaries (ep in Fig. 3A) are present, and these cells are filled with deeply stained (blue) venom granules (g) as large as 5 μm or more in diameter.

Electron microscopy confirms that the mitochondrion-rich cells with apical microvilli as described above are

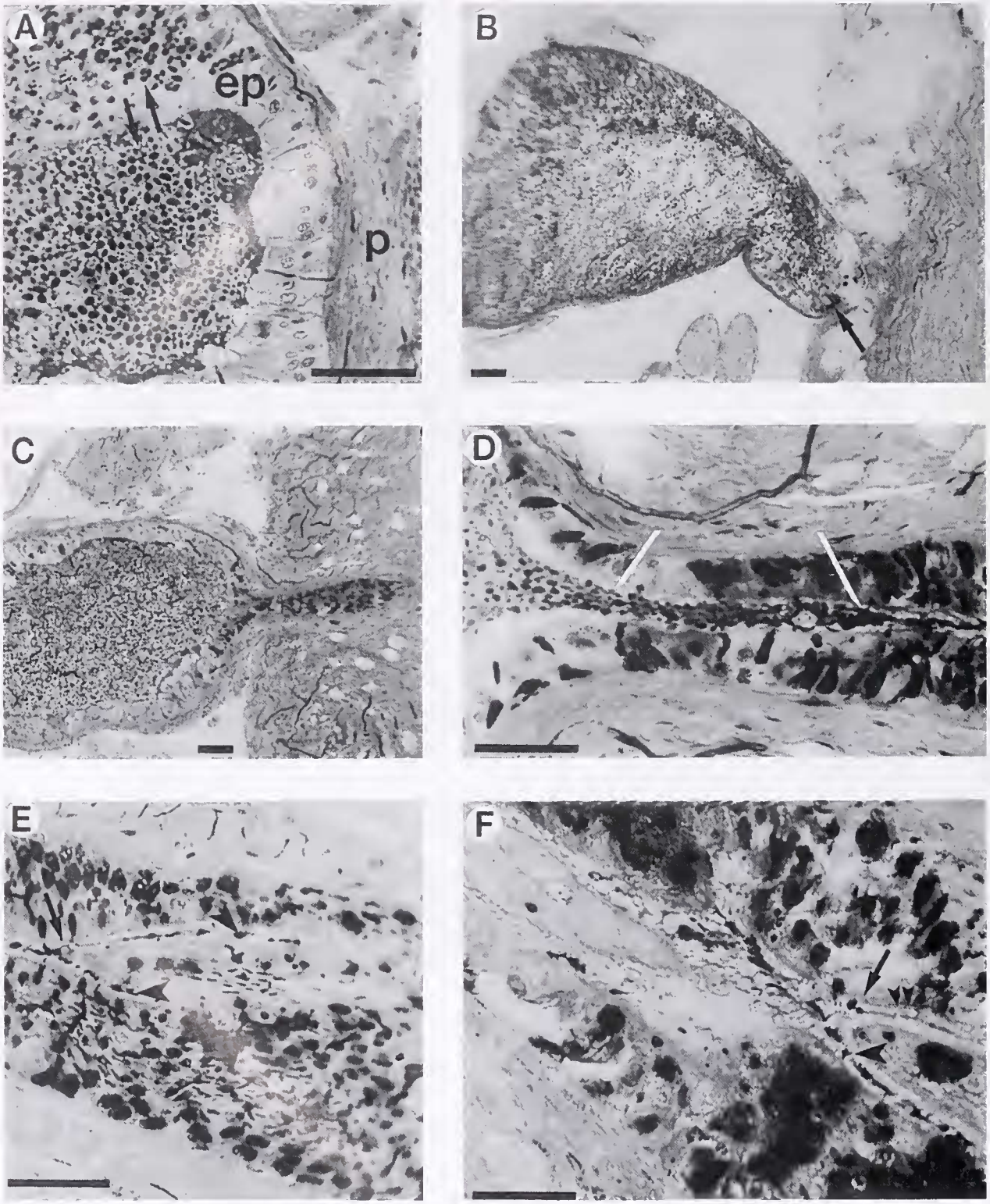

absent from this more distal region. Figure 3B shows the external border of the duct where the basal lamina (bl) separates the cellular and collagenous (c) layers that again run in at least two directions. Immediately beneath the basal lamina (bl, Fig. 3B), cross-sections of presumptive neuronal processes (nv) are sometimes found. Many of these pro-

cesses are filled with electron-dense vesicles, which are much smaller than the venom granules (g) and are not resolvable by light microscopy.

Epithelial cells just inside the external surface of the duct in this region contain numerous intracellular venom granules. A nucleus (n) and several granules can be seen within the same membrane-limited cellular unit in Figure 3C. Granules in these more peripheral epithelial cells tend to be covered with a membranous coating (small arrows). Closer to the lumen of the duct, cellular boundaries become difficult to define, even by TEM, probably because the cells are breaking down in a holocrine-type secretory process (see Halstead, 1988).

Extracellular granules well within the central duct lumen in this region are substantially more abundant than in the proximal region described above. Analysis of $50 \times 50\ \mu m^2$ areas in light micrographs at the magnification of Figure 3A yielded granule counts of 58.3 ± 48.3 (distal) *versus* 13 ± 4 (proximal; mean $\pm$ SD, $n = 3$ in both cases). Density in the distal lumen was quite variable, and the area in the upper left of Figure 3A, which was included in the analysis, is at the low end of the range (25–84).

Within this deeper region of the distal venom duct, individual venom granules display distinct ultrastructure and can be separated into at least two classes (Fig. 3D). The first (1 in Fig. 3D) has an electron-dense core surrounded by a more intensely stained ring, which in turn is covered by a diffuse coating of lightly stained material. There is no sign of the membranous coating. The second class (2) has a core that stains much more lightly, but displays a similar coating of the ring and external diffuse layer. The relationship of the two granule classes to each other or to venom production in general is not obvious from the anatomy, but presumably granules without a membranous coat derive from the clearly intracellular granules described above.

Profiles of cilia are also occasionally found in the distal lumen. In living material examined with water-immersion optics, clumps of motile cilia can be seen to create microscopic vortices but not directional fluid flow. Neither the origin nor functional significance of these processes is known.

The anteriormost venom duct and the connection to the pharynx

In general, the above description of the distal duct region applies up to its anterior end, just before it joins the pharynx, where the duct diameter is about 475 μm. Figure 4A shows an oblique, but generally longitudinal, section through this region. Some of the columnar-type epithelial cells contain intracellular granules similar to those found in the lumen of the duct (arrows), but the relative cellular *versus* luminal distribution of granules is opposite to that in Figure 3A. Here the lumen of the duct is densely packed with granules (84.7 ± 2.1 per 2500 μm^{-2}; mean $\pm$ SD, $n = 3$), and intracellular granules are sparse. Epithelial cells adjacent to the pharynx (p) appear to contain no granules at all.

As the venom duct approaches the pharynx, it narrows rapidly to a diameter of about 125 μm (Fig. 4B). At the point where the duct begins to penetrate the pharyngeal musculature, most epithelial cells resemble those cells lacking granules as described in conjunction with Figure 4A. In addition, a distinct type of smaller epithelial cell is interspersed in this region. These cells are filled with extremely small particles that are intensely stained purple by methylene blue (Fig. 4B, arrow). They are very evident in Figure 4C–F. These metachromatic "purple cells" become more numerous as the duct proceeds across the pharyngeal wall and narrows to a luminal width of about 20 μm (Fig. 4D). Venom granules in the lumen here (between white pointers in Fig. 4D) resemble those in the distal venom duct. Light- and dark-blue granules are evident in light microscopy, and they presumably correspond to the two ultrastructural classes described above.

At a distance of about 250 μm into the pharyngeal wall, the narrow venom duct passageway branches into two smaller channels, each about 10 μm wide (arrows in Fig. 4E, F). Just before the branch point, blue-stained granules are largely replaced by smaller, clear granules that continue into the finer channels. These clear granules appear to line the channel, with a few larger, stained profiles persisting in the core (single arrowheads in Fig. 4E, F). The latter objects lack the smooth profiles of venom granules, and they are

Figure 4. Anteriormost zone of distal venom duct, and the penetration of the duct into the pharyngeal wall (light micrographs). (A) Oblique section through the duct in the region of the pharynx. Epithelial cells (ep) of the duct display intracellular venom granules (upward arrow), and similar granules (downward arrow) fill the lumen as well. Epithelial cells facing the pharynx (p) do not contain granules, and prominent nuclei are evident. Scale bar is 50 μm. (B–F) Successive longitudinal sections through the venom duct as it crosses the pharyngeal wall. Scale bars are 50 μm throughout. (B) The duct as it barely penetrates the proboscis wall. At this site small epithelial cells that intensely stain purple first appear (arrow). (C) The section grazes through the metachromatic purple cells lining the venom duct as it penetrates more deeply into the pharynx. (D) Magnified view of the duct entering the pharyngeal muscle with the lumen narrowing down. Purple cells line both sides of the duct in this region. The duct becomes densely packed with blue-staining venom granules as it narrows (between white pointers). (E, F) Two views of the venom duct branching into two finer tracts inside the pharyngeal wall (arrows). Smooth, blue-staining granules (large arrowheads) become sparse after the branching point, and small, clear vesicles (small arrowheads) become more prominent and appear to line the fine channels. See text for additional details.

stained more intensely purple like the metachromatic cells. These features suggest that the stained granular material in the core of these fine channels is distinct from either of the two types of venom granules described above, but any relationship to the metachromatic cells is uncertain. In some cases, only clear granules are evident, although some amorphous material, which appears to be matted cilia, persists in the channel core (double arrowhead in Fig. 4F).

After the duct's bifurcation, each of the branches continues for about another 500 μm before opening into the lumen of the pharynx. Two such channels are visible in Figure 5A. The proximal ends are marked by ovals (the branch point is not visible in Fig. 5A), and the distal ends (stars) open into a common space connected to the pharyngeal lumen (l). Purple cells continue to line the channel epithelium to a point about halfway from the bifurcation to the distal opening. Beyond this point (bold arrows), the clear granules in the lumen of the channels become infrequent, and the passageways, which here are ciliated, grow a bit in width. The cuboidal epithelium forming the channels in this region is contiguous with the highly folded, ciliated epithelium of the pharynx. Thus, two pharyngeal folds extend particularly deeply and merge with the fine venom duct channels. It is at this junction that the novel purple cells lining the final venom duct passageway give way to the pharyngeal epithelium. A schematic summary of the nature of the venom duct as it crosses the pharyngeal wall is given in Figure 5B.

The radular sac

Teeth are manufactured in the long arm of the radular sac, but this complex region was not studied in the present work. The short arm of the radula sac is thought to contain only mature teeth that are ready for use (Marsh, 1977) and is bounded by an outer epithelial layer about 7.5 μm thick (oe in Fig. 6A), a narrow layer of connective tissue, and an inner epithelial (ie) layer composed of cells about 25 μm long. The inner epithelium is complex, highly folded, and thick (up to 125 μm in Fig. 6A).

Many radular teeth in the short arm are in close contact with this inner cellular layer. Basal spurs are easily recognized (*), and a majority of the teeth are oriented with their points towards the pharynx (Fig. 6E), but other orientations can be found (Fig. 6A,C). The space around the teeth contains a mixture of granular, cellular, and unidentifiable material, and similar materials are evident in the lumen of individual teeth (Fig. 6B). In some cases, clusters of darkly stained granules are present within the inner epithelium, and similar granules can be found inside teeth (Fig. 6D, arrows).

At the site where the teeth enter the channel passing into the pharynx, they all point anteriorly (Fig. 6E) and are enveloped by muscle of the pharyngeal wall (m). At the connection between the radular sac and the pharynx, the two structures are in intimate contact, and folds of the pharyngeal epithelium wrap around the sac (p in Fig. 6E; arrow in Fig. 6F). The packing of the basal spurs evident in Fig. 6E suggests that the teeth enter this connecting channel in a tight queue. The lumen of every tooth in this region is densely packed with a rich mixture of granules and other noncellular material (Fig. 6F).

Teeth taken from this final portion of unfixed radular sacs were also studied. Examination of such teeth under water-immersion optics confirms the presence of a large amount of granular material in the lumen (Fig. 7). This granular content does not leak out to any visually noticeable extent during several hours of observation, although FITC-dextran (fluorescein isothiocyanate-dextran, 19,000 mw) can enter the lumen and after an exchange of bathing solution can be visualized by fluorescence microscopy.

MALDI-TOF analysis of individual teeth and venom duct sections

Individual radular teeth taken from within the short arm of the radular sac, and samples of the venom duct from regions corresponding to anatomical sections 2–4 (Fig. 1), were also analyzed by mass spectrometry. Mass spectra obtained with the linear mode (positive polarity) of MALDI-TOF are illustrated in Figure 8. Reflectron-mode results were comparable (not illustrated). Although major peaks in these spectra undoubtedly represent peptide toxins, neither the amino acid composition nor the toxicity of any of these species is known. However, several general trends are evident in the distribution of peaks of specific molecular weights in different samples:

1. The most prominent peaks are not the same peptide species in different regions of the venom duct (Fig. 8A–C). The 3218 *m/z* peak is really the only one that constitutes a major presence in all three duct samples, although peaks at 2996 and 4043 *m/z* are also detectable in all samples. Most of the prominent species in the proximal duct (2275, 3370, 3460, 5088, 5285 *m/z*) are essentially absent in the distal duct samples. Methods employed in this study yield a mass accuracy for direct biological samples of typically 0.05%, and the several dalton differences between some of the peaks for the different samples shown in Figure 8 are thus insignificant.
2. The mid-distal (Fig. 8B) and anteriormost (Fig. 8C) duct samples are quite similar to one another. However, relative to the 3218 *m/z* peak, the anteriormost material appears to contain much less of the 2352 and 2525 *m/z* species and considerably more of the 4781 *m/z* peak. Many previously identified *Conus* peptides fall into this *m/z* range (Bingham *et al.*, 1996). However, due to the different composition of these sam-

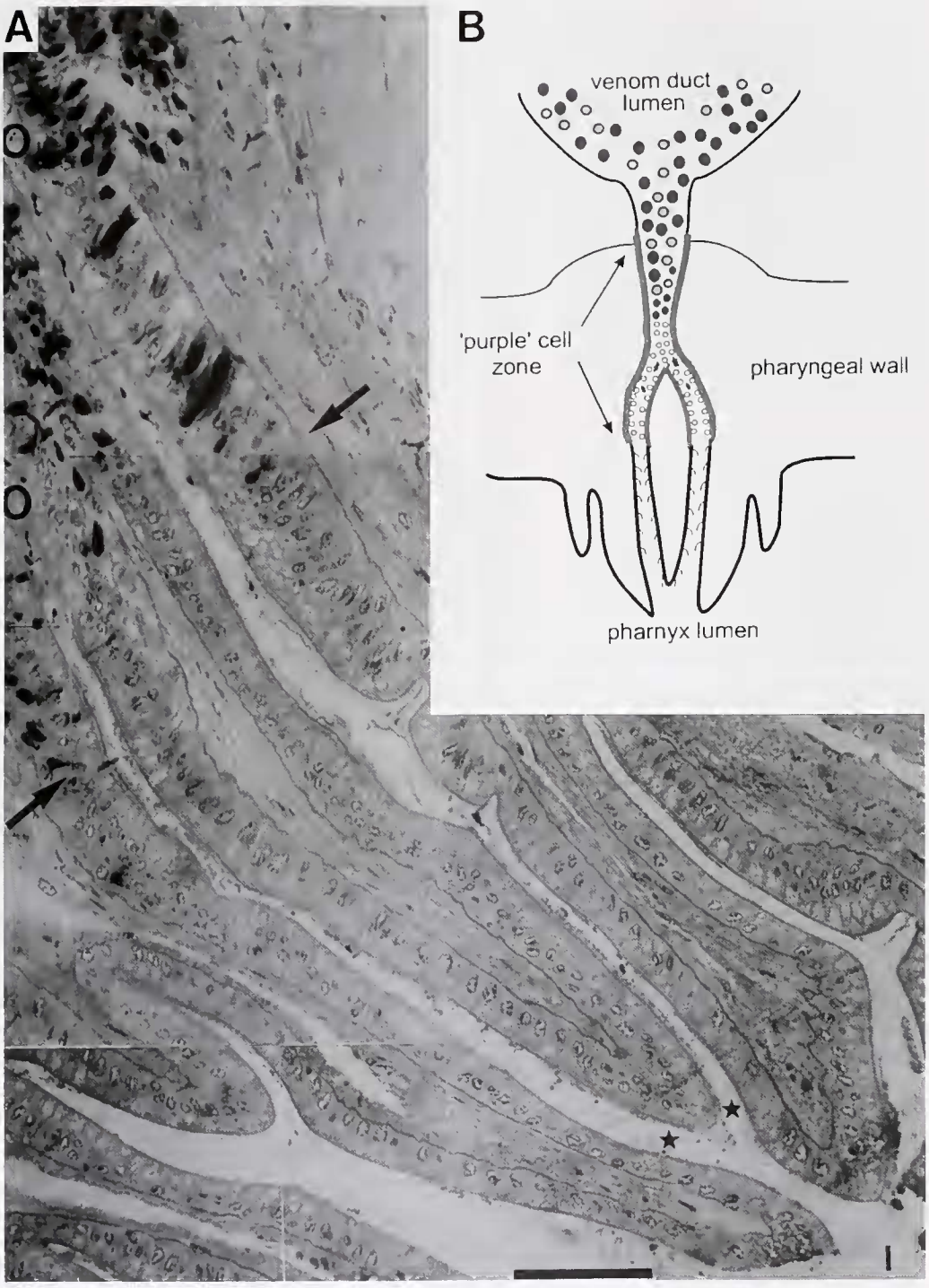

Figure 5. Longitudinal section through the fine venom duct channels as they cross the medial half of the pharyngeal wall and enter the lumen of the pharynx. (A) Ovals at the left edge of the image indicate the proximal ends of the two fine channels discussed in the text; the more proximal bifurcation where the channels are formed is not visible in this section. The two channels merge distally (*) to form a common passage that opens into the lumen of the pharynx (l). The deeply infolded pharyngeal epithelium merges proximately with the venom duct epithelium, which contains purple cells (bold arrows). Scale bar is 50 μm. (B) Schematic interpretation of the micrographs in Figures 4 and 5. See text for details. Diagram is not to scale.

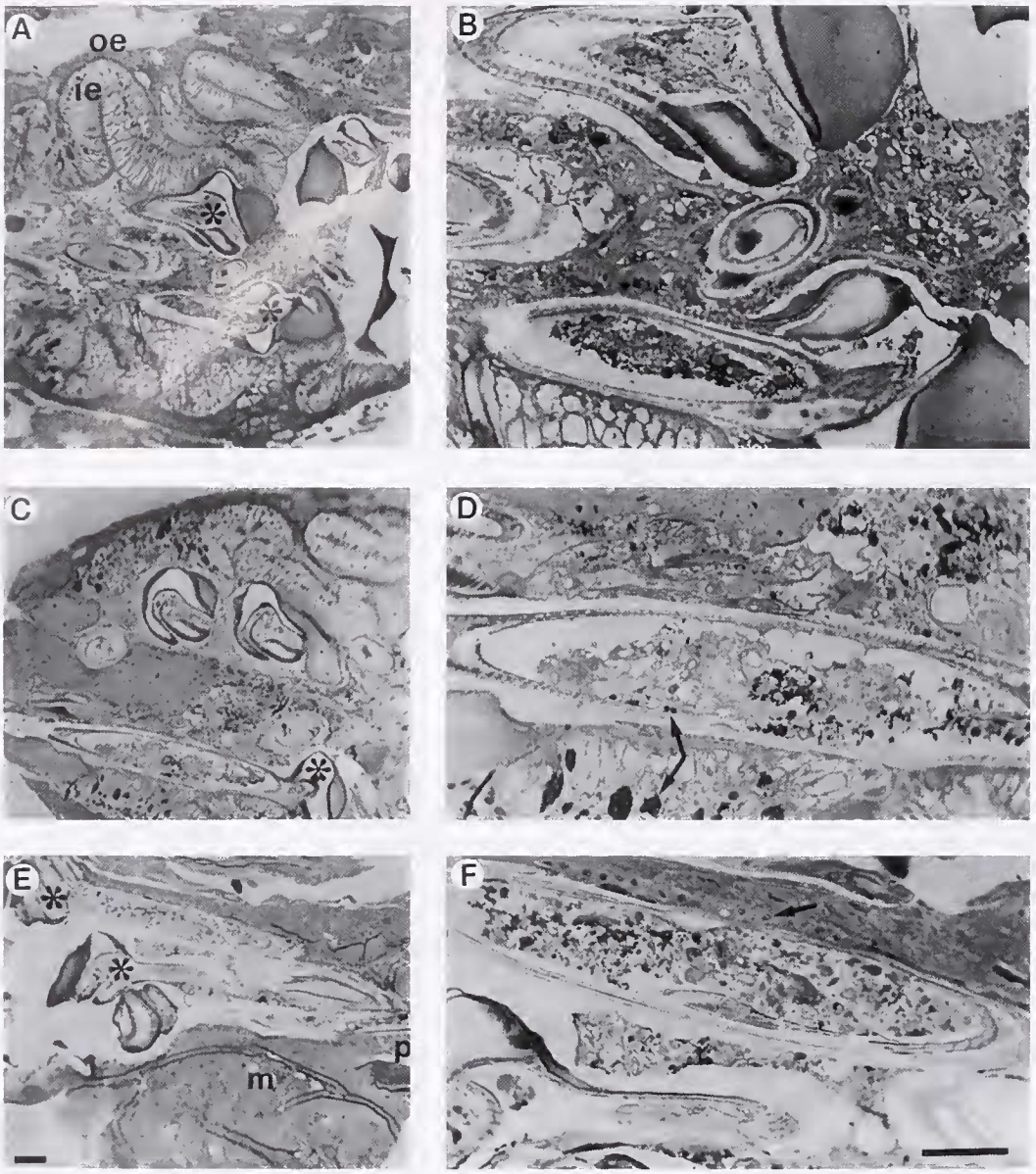

Figure 6. Short arm of the radular sac and teeth within it. Three views of teeth are shown. Each panel on the right is a magnified image of that on the left. The pharynx would be on the right side of all panels. Scale bars in E and F are 50 μm and also apply to A, C and B, D, respectively. (A, B) Comparison of radular sac content with tooth content. The basal ends (*) of two teeth are visible. Granular materials inside and outside the teeth are similar in appearance. (C, D) Dense granules (stained blue) occur in clusters within the inner epithelium of the radular sac, and similar granules are evident in the lumen of a tooth (arrows). (E, F) Three teeth in the passage through the muscle (m) of the pharyngeal wall. Pharyngeal epithelium (p [in E] and arrow [in F]) appears to line this passageway. The teeth point towards the pharynx and are all filled with granular material.

ples, the extraction and ionization efficiencies may not be identical, and this makes more quantitative comparisons of even the same peptide peak between sample types difficult.

3. The tooth sample (Fig. 8D) reveals a spectrum similar to that of the distal venom duct samples. Thus, the three most prominent peaks (2996, 3218, and 4046 *m/z*) are also present in both duct samples. However, the 4781 *m/z* peak is greatly diminished in the tooth, although it may be obscured by sodium adducts of these compounds. Although procedural differences complicate quantitative comparison of intensities between tooth and duct samples, the *m/z* values are directly comparable. Thus, these data strongly suggest that the tooth lumen contains some, but perhaps not all, of the peptides found in the venom duct.

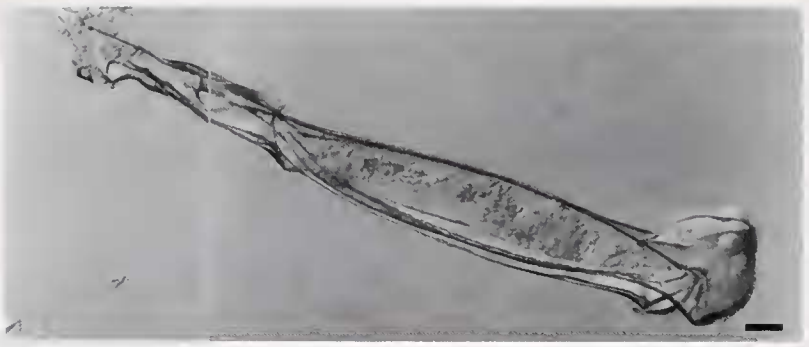

Figure 7. Non-fixed tooth dissected from the short arm of the radular sac at the site closest to the pharynx (*i.e.*, as in Fig. 6E, F) and examined with water-immersion optics. Granular material in the lumen is clearly visible. Connective tissue at the tip of the tooth was not always present. Scale bar is 50 μm.

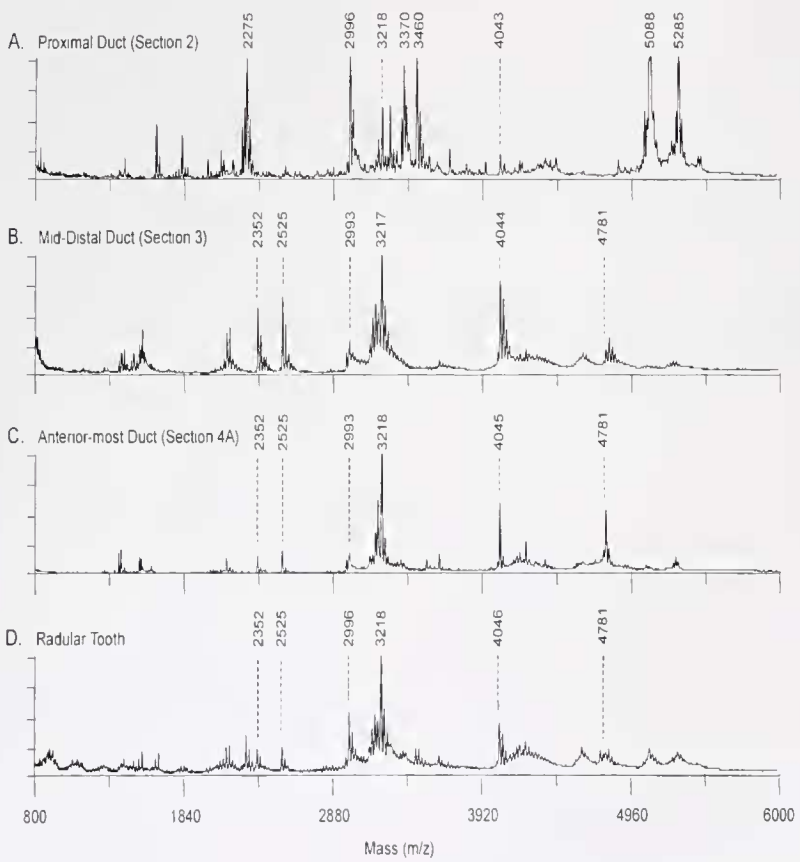

Figure 8. Representative mass spectra (MALDI-TOF) for selected regions of the venom duct and for a single tooth from the short arm of the radular sac. (A) Proximal venom duct (corresponding to section 2 in Fig. 1). (B) Mid-distal venom duct (section 3 in Fig. 1). (C) Anteriormost venom duct (section 4A in Fig. 1). (D) Luminal contents of tooth. Presumptive peptide peaks from the tooth are a subset of those contained in venom duct. See text for additional details. Comparable spectra were obtained from other radular teeth from the same snail (not illustrated).

Discussion

As described in this paper, the general anatomy of the venom apparatus of *Conus californicus* is similar to that in other *Conus* species. This is noteworthy, because *C. californicus* is an atypical member of the genus. The vast majority of tropical species, including all of those previously studied anatomically, are highly specific for certain prey types (Kohn, 1956, 1966; Nybakken, 1970, 1990). However, *C. californicus*, a temperate species, is a generalized feeder (Kohn, 1966) with unusual radular teeth (Kohn *et al.*, 1999) and a variety of feeding strategies (Saunders and Wolfson, 1961).

Along with the general anatomical similarities, we have identified several features in *C. californicus* that have not been described in other species. Whether these features are characteristic of other *Conus* species remains to be established:

1. The proximal venom duct is composed of a well-organized epithelium that is highly specialized, and the lumen contains a great deal of cellular debris and few venom granules.
2. The distal venom duct is composed of a poorly organized epithelium. The lumen contains both cellular debris and many venom granules.
3. The connection between the venom duct and the pharynx is a complex, branching channel that is extremely narrow for most of the distance across the pharyngeal wall. A unique type of epithelial cell is found only in this region.
4. Teeth within the radular sac contain luminal granular material, and mass spectrometry reveals putative peptides in the tooth lumen that are also found in the venom duct.

The proximal venom duct

Previous studies have indicated that material extracted from the proximal portion of the *Conus* venom duct has different peptides (Bingham *et al.*, 1996), venom granules, and pharmacological properties (Endean and Duchemin, 1967) than that extracted from the distal duct. However, the role of this region in venom production remains vague, and no anatomical specialization suggestive of a secretory function has been reported.

TEM images described in this paper reveal that the proximal duct is structurally unique. The high concentration of mitochondria found in the basal region of the epithelial cells must be associated with a high level of energy production, and microvilli greatly increase the apical surface area. Although both features might be associated with secretion, there are no other structural aspects of these cells that support this idea.

In contrast, the above structural features suggest that this tissue mediates active transport. In particular, the epithelium of the proximal venom duct is strikingly similar to the proximal tubule of the mammalian kidney. The latter epithelium absorbs glucose and amino acids along with sodium through apical microvilli and actively transports sodium into the bloodstream across the basal surface with energy provided by numerous mitochondria. Although the nature of the postulated transport process in the proximal venom duct is unknown, it is possible that this epithelium functions in a similar manner to take up ions and small organic molecules (*e.g.*, amino acids, fatty acids) from the duct lumen as part of a recycling mechanism. An attractive source for these molecular substrates is the prominent cellular debris in the lumen.

The distal venom duct

Few venom granules or obvious precursor materials exist in the lumen of the proximal duct, and this suggests that venom granules are manufactured elsewhere, presumably in more anterior duct regions. Numerous venom granules characterize the entire distal venom duct, and they are found both within epithelial cells and in the lumen. Over the length of the distal duct, the relative abundance of granules changes from primarily intracellular proximally to extracellular distally. Cellular debris is also abundant in the lumen of the initial segment of the distal duct (*i.e.*, the more posterior region).

These features strongly suggest that venom granules originate in the distal venom duct. The epithelial cells of this region probably express the genes encoding specific peptides, and granules appear to be assembled in the same cells. The disorganized nature of this epithelium, the poorly defined cell membranes, and the cellular debris in the lumen are all consistent with holocrine secretion, as suggested by previous authors (Halstead, 1988; see also dos Santos *et al.*, 2000). Thus, the abundant cellular debris in the lumen of the proximal duct probably derives from this distal secretory region.

Our analysis of *C. californicus* contrasts somewhat with work on *C. magus* by Endean and Duchemin (1967) in which "immature" venom granules were identified within the distal duct and extremely large "mature" granules (up to 20 μm long and 5 μm wide) were found in the proximal duct. On the basis of the presumed developmental progression, those authors suggested that granules did not originate in the posterior duct. Although we agree with that conclusion, we find few granules of any sort in the proximal duct and no extremely large granules anywhere in *C. californicus*. Reasons for these differences are not clear, and subcellular anatomical studies on other species are inadequate to permit a meaningful comparative analysis.

The connection between the venom duct and proboscis

An important contribution of this paper is the description of the passageway taken by the venom duct into the pharynx (see Fig. 5C). Two features of this region are likely to be important to the manufacture and delivery of venom.

First, the venom duct narrows to channels only 10 μm or less in width as they cross the pharyngeal wall. This appearance can last through 100 μm of serial sections cut parallel to the long axis of the passage. This suggests that the passage is not a cylindrical duct, but rather a flat channel that is much larger in one dimension than the other. The course of these channels becomes somewhat convoluted after the bifurcation, making it impossible to capture the entire length across the pharynx in a single section. Thus, the number of such channels is uncertain, but there are at least two. These channels merge once again upon reaching the lumen of the pharynx, and presumably this is where venom enters the pharynx *in vivo* (* in Fig. 5A).

The small diameter and considerable length of the fine connecting channels suggest that venom ejection is not likely to involve high flow rates or large volumes. Possibly the cilia lining the distal portions of the fine channels are involved in transport of venom into the pharynx (see also below). A very narrow opening into the pharynx and an associated ciliated tuft were also described in *C. magus* (Endean and Duchemin, 1967), but the passage within the pharyngeal wall was not elaborated upon.

The second important feature is the unique type of epithelial cell that surrounds the fine duct channels over their course through the pharyngeal wall. These metachromatic cells, which we call purple cells, appear in the wall of the duct just before it enters the pharynx, and they line the passageway to the point at which this epithelium meets the infolded pharyngeal epithelium (see Fig. 5B). The specialized nature and localization of the purple cells suggest that they play a critical role in the production or delivery of venom. It is possible that these cells are secretory and contribute a specific component to the final venom for ejection. Such components could be peptides not found elsewhere in the venom duct (Bingham *et al.*, 1996), enzymes such as phospholipases (McIntosh *et al.*, 1995), or simply mucus.

Alternatively, the purple cells could play an active role in "simplifying" venom from the duct in preparation of the final material to be injected into a victim. Venom "milked" from living *Conus* of several species contains a much simpler complement of peptidic toxins than that found in crude venom isolated from the duct (Hopkins *et al.*, 1995; Bingham *et al.*, 1996). Our anatomical data suggest that some kind of granule breakdown or sorting process may occur in the fine channels of the venom duct, because at the final branching point, large blue granules are replaced by smaller, clear ones (Fig. 4D–F). Purple cells might selectively take up materials or release specific products that act to break down or modify the granules. In turn, this action could lead to simplification of the peptide complement of the final venom. The purple-cell zone may well represent the site of this process, but the underlying biochemical mechanisms remain to be elucidated.

The radular sac and teeth

As demonstrated in this paper, radular teeth of *C. californicus* are filled with a rich assortment of granules and other material. This is true for teeth well within the short arm of the radular sac as well as those that are ready to be passed to the proboscis. Examination of non-fixed teeth confirms the presence of granular material. Morphological similarities with material in the lumen of the venom duct make it plausible that peptide toxins exist in both places. This idea is directly supported by mass spectrometry analysis. Thus, *C. californicus* teeth in the radular sac appear to be "pre-loaded" with peptidic components of venom before being passed to the proboscis for use in hunting. This hypothesis obviously contrasts with the ideas discussed in the Introduction.

A summary model for venom manufacture and delivery in Conus californicus

Profound ultrastructural differences between the proximal and distal portions of the venom duct suggest major functional differences for these regions. We propose that peptide toxins are synthesized and assembled into venom granules within the epithelial cells of the distal venom duct, and that the contents of these cells are discharged into the lumen of the duct, probably by holocrine secretion. Cellular debris resulting from this process would be recycled through an uptake pathway in the proximal venom duct. If so, the muscular bulb may play some role in the reuptake process.

Venom granules are extremely abundant in the lumen of the anteriormost region of the distal venom duct. However, they are prevented from free passage into the pharynx by the network of specialized narrow channels that connects the duct and the pharynx. Slow and limited transport of venom probably occurs across these channels, and some material may be directed into the radular sac, where teeth can be loaded with at least some venom components. This postulated transport need not involve a complex mechanism, and a specialized ciliary tract in a typhlosole-like structure could easily move the requisite material along the highly folded pharyngeal epithelium and into the radular sac.

During the slow passage of venom through the fine duct channels in the purple-cell zone, the granule content and peptide complement of the crude venom could be simplified as hypothesized above. This simplification would appear to be a requirement for *in vivo* preparation of the final venom

for injection. This important feature is difficult to explain if large volumes of material from the anterior venom duct are quickly passed into the pharynx.

Finally, our model is compatible with the possibility that venom injection involves more material than could be contained in the lumen of a single tooth. We are unaware of quantitative data demanding this capability for any *Conus* species, but it seems likely to be true. Neuronal control over the richly innervated pharyngeal musculature might permit sufficient dilation of the fine duct channels to move a bit of extra venom into the pharynx once the pre-loaded tooth was passed from the radular sac. This bolus of venom could be carried along at the base of the tooth to the tip of the proboscis for final ejection. In this case, if the extra venom were limited to the material of unique granular content contained in the narrow channels, it could still retain a simplified peptide composition.

Acknowledgments

We are grateful to Chris Patton of Hopkins Marine Station for assistance with TEM sectioning, other microscopic techniques, and photographic work. We thank Dr. Joseph Schulz for critically evaluating the manuscript, and Drs. Barbara Block, Simon Hathaway, and William C. Pitts for helpful suggestions. This work was partially supported by a Stanford University Undergraduate Research Opportunity award sponsored by the Howard Hughes Medical Institute to J.M., by NIH grants NS-17510 (W.F.G.) and NS-31609 (J.V.S.), and by NSF grant IBN-0131788 (W.F.G.).

Literature Cited

Bergh, R. 1895. Beiträge zur Kenntniss der Coniden. *Nova Acta Leopold.* **65**(2): 69–214.

Bingham, J.-P., A. Jones, R. J. Lewis, P. R. Andrew, and P. F. Alewood. 1996. *Conus* venom peptides (conopeptides): inter-species, intra-species and within individual variation revealed by ionspray mass spectrometry, Pp. 13–27 in *Biomedical Aspects of Marine Pharmacology,* E. Lazarovici, M.E. Spira, and E. Zlotkin, eds. Alaken, Fort Collins, CO.

Bingham, J.-P., A. Burlingame, E. Moczydlowski, and W. F. Gilly. 2000. A new highly selective conotoxin from *Conus californicus* that targets voltage-gated neuronal Na^+ channels of squid. *J. Gen. Physiol.* **116:** 12A.

Conticello, S. G., Y. Gilad, N. Avidan, E. Ben-Asher, Z. Levy, and M. Fainzilber. 2001. Mechanisms for evolving hypervariability: the case of conopeptides. *Mol. Biol. Evol.* **18:** 120–131.

Cottrell, G. A., and B. M. Twarog. 1972. Active factors in the venom duct of *Conus californicus*. *Br. J. Pharmacol.* **44:** 365P–366P.

dos Santos, V. L. P., C. R. V. Franco, R. L. L. Viggiano, R. B. da Silveira, M. P. Cantao, O. C. Mangili, S. S. Veiga, and W. Gremski. 2000. Structural and ultrastructural description of the venom gland of *Loxosceles intermedia* (brown spider). *Toxicon* **38:** 265–285.

Duda, T. F., and S. R. Palumbi. 1999. Molecular genetics of ecological diversification: duplication and rapid evolution of toxin genes of the venomous gastropod *Conus*. *Proc. Natl. Acad. Sci. USA* **96:** 6820–6823.

Elliot, E. J., and J. Kehoe. 1978. Cholinergic receptors in *Aplysia* neurons: activation by a venom component from the marine snail *Conus californicus*. *Brain Res.* **156:** 387–390.

Elliot, E. J., and M. A. Raftery. 1979. Venom of marine snail *Conus californicus*: biochemical studies of a cholinomimetic component. *Toxicon* **17:** 259–268.

Endean, R., and C. Duchemin. 1967. The venom apparatus of *Conus magus*. *Toxicon* **4:** 275–284.

Freeman, S. E., R. J. Turner, and S. R. Silva. 1974. The venom and venom apparatus of the marine gastropod *Conus striatus* Linne. *Toxicon* **12:** 587–592.

Greene, J. L., and A. J. Kohn. 1989. Functional morphology of the *Conus* proboscis (Mollusca: Gastropoda). *J. Zool. Lond.* **219:** 487–493.

Halstead, B. W. 1988. *Poisonous and Venomous Marine Animals of the World.* Darwin Press, Princeton, NJ. Pp. 243–263.

Hermitte, L. C. D. 1946. Venomous marine molluscs of the genus *Conus*. *Trans. R. Soc. Trop. Med. Hyg.* **39:** 485–512.

Hinegardner, R. T. 1958. The venom apparatus of the cone shell. *Hawaii Med. J.* **17:** 533–536.

Hopkins, C., M. Grilley, C. Miller, K. Shon, L. J. Cruz, W. R. Gray, J. Dykert, J. Rivier, D. Yoshikami, and B. M. Olivera. 1995. A new family of *Conus* peptides targeted to the nicotinic acetylcholine receptor. *J. Biol. Chem.* **270:** 22361–22367.

Kohn, A. J. 1956. Piscivorous gastropods of the genus *Conus*. *Proc. Natl. Acad. Sci.* **42:** 168–172.

Kohn, A. J. 1966. Food specialization in *Conus* in Hawaii and California. *Ecology* **47:** 1041–1043.

Kohn, A. J. 1998. Superfamily Conoidae. Pp. 846–854 in *Mollusca: The Southern Synthesis. Part B. Fauna of Australia,* Vol. 5. P. L. Beesley, G. J. B. Ross, and A. Wells, eds. CSIRO Publishing, Melbourne.

Kohn, A. J., and C. Hunter. 2001. The feeding process in *Conus imperialis*. *Veliger* **44:** 232–234.

Kohn, A. J., M. Nishi, and B. Pernet. 1999. Snail spears and scimitars: a character analysis of *Conus* radular teeth. *J. Molluscan Stud.* **65:** 461–481.

Kohn, A. J., P. R. Saunders, and S. Weiner. 1960. Preliminary studies on the venom of the marine snail, *Conus*. *Ann. NY Acad. Sci.* **90:** 706–725.

Li, L., R. W. Garden, and J. V. Sweedler. 2000. Single-cell MALDI: a new tool for direct peptide profiling. *Trends Biotechnol.* **18:** 151–160.

Maguire, D., and J. Kwan. 1992. Cone shell venoms—synthesis and packaging. Pp. 11–18 in *Toxins and Targets: Effects of Natural and Synthetic Poisons on Living Cells and Fragile Ecosystems*, D. Watters, M. Lavin, D. Maguire, and J. Pearn, eds. Harwood Academic Publishers, Philadelphia.

Marsh, H. 1977. The radular apparatus of *Conus*. *J. Molluscan Stud.* **43:** 1–11.

McIntosh, J. M., F. Ghomashchi, M. H. Gelb, D. J. Dooley, S. J. Stoehr, A. B. Giordani, S. R. Naisbitt, and B. M. Olivera. 1995. Conodipine-M, a novel phospholipase A_2 isolated from the venom of the marine snail *Conus magus*. *J. Biol. Chem.* **270:** 3518–3526.

McIntosh, J. M., A. D. Santos, and B. M. Olivera. 1999. *Conus* peptides targeted to specific nicotinic acetylcholine receptors subtypes. *Annu. Rev. Biochem.* **68:** 59–88.

Nybakken, J. 1970. Correlation of radula tooth structure and food habits of three vermivorous species of *Conus*. *Veliger* **12:** 316–318.

Nybakken, J. 1990. Ontogenetic change in the *Conus* radula, its form, distribution among the radula types, and significance in systematics and ecology. *Malacologia* **32:** 35–54.

Olivera, B. M. 1997. *Conus* venom peptides, receptor and ion channel targets, and drug design: 50 million years of neuropharmacology. *Mol. Biol. Cell* **8:** 2101–2109.

Olivera, B. M., D. R. Hillyard, M. Marsh, and D. Yoshikami. 1995.

Combinatorial peptide libraries in drug design: lesson from venomous cone snails. *Trends Biotechnol.* **13:** 422–426.

Röckel, D., W. Korn, and A. J. Kohn. 1995. *Manual of the Living Conidae. Vol. 1. Indo-Pacific Region.* Verlag Christa Hemmen, Wiesbaden, Germany. 517 pp.

Saunders, P. R., and F. Wolfson. 1961. Food and feeding behavior in *Conus californicus* Hinds, 1844. *Veliger* **3:** 73–76.

Shaw, H. Q. 1914. On the anatomy of *Conus tulipa* Linn., and *Conus textile* Linn. *Q. J. Microsc. Sci.* **60:** 1–60.

Songdahl, J. H. 1973. The venom and venom apparatus of the Atlantic cone, *Conus spurius atlanticus* (Clench). *Bull. Mar. Sci.* **23:** 600–612.

Spengler, H. A., and A. J. Kohn. 1995. Comparative external morphology of the *Conus* osphradium. *J. Zool. (Lond.)* **235:** 439–453.

Sweedler, J. V., L. Li, P. Floyd, and W. Gilly. 2000. Mass-spectrometric survey of peptides in cephalopods with an emphasis on the FMRFamide-related peptides. *J. Exp. Biol.* **203:** 3565–3573.

Whysner, J. A., and P. R. Saunders. 1963. Studies of the venom of the marine snail *Conus californicus. Toxicon* **1:** 113–122.

Whysner, J. A., and P. R. Saunders. 1966. Purification of the lethal fraction of the venom of the marine snail *Conus californicus. Toxicon* **4:** 177–181.